Investigation of Properties of Synthetic Microparticles for a Retention and Drainage System

Sa Yong Lee*, Martin A. Hubbe†, and Sunkyu Park‡

*Graduate Student, †Associate Professor, ‡ Research Associate in Univ. of Tennessee
Department of Wood and Paper Science, North Carolina State University,
Campus Box 8005, Raleigh, NC 27695-8005, USA
hubbe@ncsu.edu

ABSTRACT

Over the past 20 years there has been a revolution involving the use of nano or macro size particles as drainage and retention systems during the manufacture of paper. More recently a group of patented technologies called Synthetic Mineral Microparticles (SMM) has been invented and developed. This system has potential to further promote the drainage of water and retention of fine particles during papermaking. Prior research, as well as our own preliminary research showed that the SMM system has advantages in both of drainage and retention, compared with montmorillonite (bentonite), which one of the most popular materials presently used in this kind of application. In spite of the demonstrated advantages of this SMM system, the properties and activity of SMM particles in the aqueous state have not been elucidated yet.

Streaming current titrations with highly charged polyelectrolytes were used to measure the charge properties of SMM and to understand the interactions among SMM particles, fibers, fiber fines, and cationic polyacrylamide (cPAM) as a retention aid. It was found that pH profoundly affects the charge properties of SMM, due to the influence of Al-ions and the Si-containing particle surface. SEM pictures, characterizing the morphology, geometry and size distribution of SMM, showed a broad distribution of primary particle size. Dilution of SMM mixtures appeared to wash out particles smaller than 100 nm from the surface of larger particles, which themselves appeared to be composed of fused primary particles. DSC thermoporometry was used to measure the size distribution of nanopores within SMM particles.

INTRODUCTION

Microparticulate retention and drainage aid systems for papermaking have become increasingly popular, starting in the early 1980s. Bentonite is one of the most popular microparticle types used in this type of application [1].

Bentonite is being used together with high-mass cationic polyelectrolytes to promote retention and drainage as the paper web is being formed. The width of a bentonite particle is almost as large as mineral fillers used in papermaking or as pigments used in coating formulations, but the thickness can be less than 20 nm [2-5].

Colloidal silica is the other popular microparticle type. According to Iler [6], these particles generally fall into two major classes, "sol" and "gel." "Sol" means that the primary particles exist separately from each other, whereas "gel" means that the primary particles have coagulated and fused together into chains or clusters during their preparation. Sol-type colloidal silica products have been used as papermaking additives from the 1980s [7-8]. Gel-type colloidal silica products have been used at least since the 1990s [9-12].

Highly cross-linked water-soluble polymers called micropolymers have been used to obtain the similar effects as with bentonite and colloidal silica [11,13-15]. Like their mineral counterparts, the micropolymers have high negative charge density. They also can be highly efficient, employing a smaller amount on a mass basis to get a certain degree of retention and drainage, compared with other microparticles.

Synthetic Mineral Microparticles (SMM)

During the last 10 years a collection of patented technologies called "Synthetic Mineral Microparticles" (SMM) has been invented and developed to further increase the retention of fine materials used in paper manufacturing and to increase the rate of drainage, allowing further increases in production rates [16-18].

The SMM technology is protected by the following US patents: US 6,184,258, process for preparation of microparticles [16]; US 5,989,714, composition patent for microparticles [17]; and US 6,183,650, water treatment by means of microparticles [18]. US 6,184,258 describes the most basic invention, showing that highly effective microparticles can be synthesized by simple mixing a dilute solution of silicate ions and a dilute solution of aluminum ions. This procedure is very similar to the synthesis used in the present study..

The SMM product can be envisioned as being a composite of small parts, based on a precipitation reaction between metal ionic species and silicate ions. The chemical process of synthesizing SMM can be illustrated

by the following reaction between sodium metasilicate (SMS) and aluminum sulfate (alum):

$$y\mathrm{Na_2SiO_3} + x\mathrm{Al_2(SO_4)_3} \rightarrow \mathrm{Na_{2y-6x}Al_{2x}Si_yO_{3y}} + 3x\mathrm{Na_2SO_4}$$

As disclosed in the patents, the chemical nature of the additives and their relative concentrations in the mixture can be varied within relatively wide ranges.

The relative simplicity of SMM preparation allows certain advantages, such as on-site preparation, reduced cost, good retention and dewatering performances, an ability to optimize microparticle properties needed during paper production, and a more favorable balance of retention and paper uniformity.

Even though this SMM system has some demonstrated advantages, the properties and activities of SMM in the aqueous state have not been elucidated yet. In this paper, the properties of SMM for the drainage and retention enhancement will be investigated with respect to the following factors: (1) colloidal charge density of SMM mixtures, (2) pore size distribution within the particles, and (3) morphological characters of the particles, depending on the synthetic conditions such as Al/Si ratio, salt, shear rate, and the effect of partial neutralization of the alum with NaOH. The results of this study provide information that can be helpful for those who prepare microparticles, as well as for papermakers, regarding the SMM technique and the optimum conditions to apply it in papermaking as a retention and drainage system.

EXPERIMENT

Materials

SMM suspensions were synthesized in a manner consistent with the patents [16-18]. Sodium meta-silicate ($Na_2SiO_3 \cdot 5H_2O$) was used as base ingredient with 0.445 molal concentration. The added metal solution ingredient was 0.566 molal aluminum chloride ($AlCl_3$). This compound was selected, based on environmental and industrial concerns, from among various other compounds included within the patent claims.

The synthetic factors constituting this study were as follows:

- Constants
  - Na_2SiO_3 : 0.455 molal solution
  - $AlCl_3$: 0.566 molal solution
  - Shear rate : 13,000 rpm
- Variables
  - Al/Si ratios : 0.50 / 0.63 / 0.76 / 0.88 / 1.00
  - Salt : None / 1mM NaCl
  - Neutralization : None / 25% with 1N NaOH

The percent neutralization was defined as the ratio of added NaOH to $AlCl_3$, on a molar basis. Partially neutralized aluminum-containing solutions were used for microparticle preparation, in place of pure $AlCl_3$ solutions. Polyvinylsulfate, potassium salt (PVSK, Aldrich 27,196-9, Mw = Ca. 170,000) and poly-diallyldimethyl-ammonium chloride (P-DADMAC, Aldrich 40,901-4, Mw = Ca. 100,000 ~ 200,000) were used as titrants for measuring charge densities of SMM preparations.

Measurement of Charge Densities of SMM

An SMM suspension was prepared, using the synthesis procedure described in the patents [16-18]. A commercial blender was used to achieve a 13,000 rpm level of agitation. The pH of the suspension was measured after synthesis.

For measuring the charge density, 10g of suspension was taken in a 200 ml beaker and diluted 5 times to 50g with deionized water. The pH of the diluted suspension was also measured. Titration was then performed on the diluted suspension. The weight concentration of solid was measured accurately by Thermogravimetric Analysis (TGA) for calculation of a charge density per unit solid mass of the suspension.

To measure the charge densities of particles and ionic species, 10g of microparticle suspension was placed in a centrifuge cell and diluted 5 times to 50g with deionized water. The pH value of diluted suspension was also measured, and the diluted mixture in the cell was centrifuged. The supernatant was collected in another tared centrifuge cell. The mass and pH of the collected supernatant were recorded. The titration was performed subsequently. The mass concentration of supernatant was measured by TGA.

Deionized water was added to bring the total mass to 50 g in the centrifuge cell, which had the centrifuged solid from the SMM suspension. The solid in that cell was dispersed again with a vortex generator and ultra-sonicator. Titration subsequently was performed on the redispersed suspension and the pH was measured. The mass concentration of solid in centrifuge cell was measured accurately by TGA for calculation of a charge density of the redispersed suspension.

Pore Size Distribution of SMM

Pore size distributions within the SMM particles were characterized by differential scanning calorimetry (DSC) [19-20]. In order to remove salt effects, cleaned samples were prepared from synthesized SMM suspensions to remove freezing point depression caused by salt. At first, 50 g of SMM suspension was taken and centrifuged with 1174 g of centrifuge force and 10 min of centrifuge time. The supernatant was replaced with deionized water. The sample then was redispersed by vortex generator. This cleaning was repeated 3 times. Centrifugal filtering was performed with 15 g of cleaned sample, using an Amicon Ultra-15 centrifugal filter device (100K NMWL) in order to reduce the moisture ratio of the microparticle mixture. The centrifuge force was 873 g and the time of centrifugation was 10 min.

The prepared microparticle sample was cooled to -30°C in the DSC device and maintained for 5 min and the temperature was then raised to -25°C at 1°C/min. This first segment (-30 ~ -25°C) was used to determine the sensible heat of the mixture, assuming that there was no melting. Subsequent heating steps to slightly higher

temperatures (-20, -15, -10, -8, -6, -5, -4, -3, -2, -1.7, -1.4, -1.1, -0.9, -0.7, -0.5, -0.3, -0.2, -0.1°C) were then performed in succession. In each step, the temperature was raised at 1°C/min to the target temperature and then the sample was maintained isothermally until the heat flow returned to the baseline. Detailed procedures can be found elsewhere [21-23].

The amount of water that has its melting temperature depression at each isothermal step in the procedure was calculated by integrating the endotherm. Each endotherm represents a specific pore diameter, based on the Gibbs-Thomson equation, Eq. (1). The relationship between a pore diameter (D) and the depressed melting temperature (T_m) has been described previously [24]. The use of this equation is based on the assumption that the microparticles are not soluble in the water and that it is useful to model their pores as ideal cylinders,

$$\Delta T = T_0 - T_m = \frac{-4T_0\gamma_{ls}}{D\rho H_f} \quad (1)$$

$$\gamma_{ls} = 20.36\times10^{-3}(1-15.90\times10^{-3}\Delta T) \quad (2)$$

$$\rho(T) = -7.1114+0.0882\cdot T-3.1959\times10^{-4}\cdot T^2+3.8649\times10^{-7}\cdot T^3 \quad (3)$$

where T_0 is the melting temperature of water (273.15 K), H_f is the specific heat of fusion of freezing bound water which is assumed to be the same as that of unbound water (334 J/g) [23,25], D is the diameter of a certain pore, and ΔT is the melting temperature depression (K). γ_{ls}, the surface energy at the ice-water interface, is treated as a function of temperature, and it is calculated by Eq. (2). The density of water ρ also was treated as a function of temperature, using Eq. (3) [20].

Thus, water held in a smaller pore has a larger melting temperature depression. Average pore size was calculated based on the pore size distribution measured using DSC.

Morphology of Microparticles by Means of Scanning Electron Microscopy

Samples were prepared and imaged in two ways:

1. Prepared SMM mixtures were filtrated centrifugally, using Amicon Ultra-15 centrifugal filters (100K NMWL). The centrifuge force was 873 g, and the duration was 10 min. Filtrated thick paste samples were spread on mica surfaces and dried under vacuum overnight. Finally, the top surface was coated with gold and placed in either an environmental scanning electron microscope (E-SEM: Hitachi S-3200 Scanning Electron Microscope) or a field emission scanning electron microscope (FE-SEM: JEOL 6400F Field Emission SEM).

2. Synthesized microparticle suspensions were diluted 50 times with deionized water to investigate the morphology of aggregated structure under conditions more similar to real usage. Diluted suspensions were dropped onto the surface of mica and dried in a vacuum dryer overnight. Finally, the top surface was coated with gold and placed in a field emission scanning electron microscope (FE-SEM: JEOL 6400F Field Emission SEM).

RESULTS AND DISCUSSION

Charge Densities of SMM Suspension, Particles, and Ionic species

Figure 1(a) shows charge densities based on total solids in suspensions of microparticles. As described earlier, the polyelectrolyte titrations employed streaming current measurements for endpoint detection. Results were separated into two groups, depending on whether NaOH had been added to the aluminum additive before preparation of the microparticles (25% neutralized). In the case of non-neutralized conditions, the net charges of the resulting suspensions changed from negative to positive at an Al to Si ratio between 0.64 and 0.76. In the case of 25% neutralization, the changes in sign were shifted to ratios between 0.76 and 0.88 Al/Si. The effects of salt additions were not as significant, compared to tests carried out in the absence of NaOH.

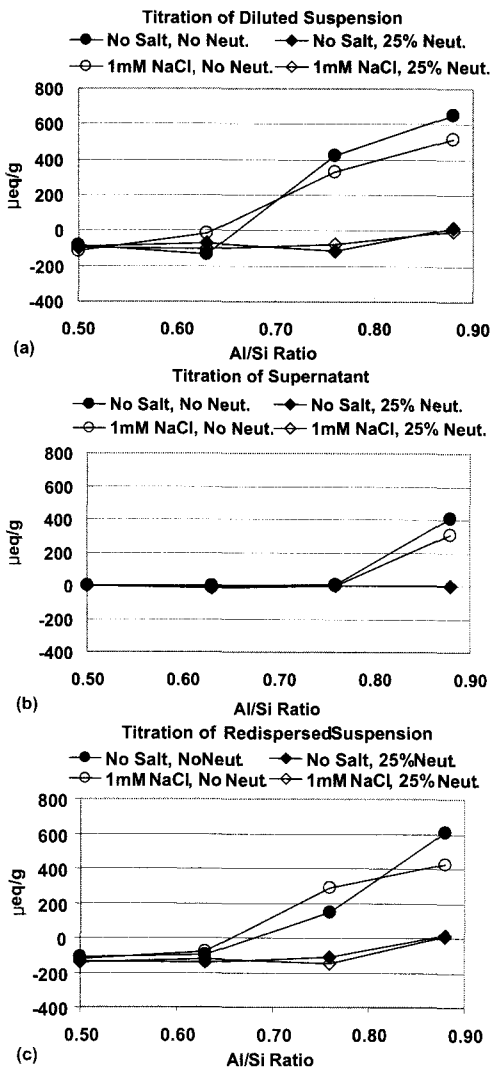

Fig. 1. The charge densities of SMM suspensions, including residual chemicals *vs.* Al/Si ratios: (a) diluted suspension; (b) supernatant; (c) redispersed suspension.

Figure 1(b) shows the charge densities of supernatant solutions. These values are attributed to the interactions of the polyelectrolyte titrants with residual ionic species in the supernatant solutions. As shown, all of the data lay under, but very near to zero, except for two points corresponding to 0.88 Al/Si, non-neutralized conditions.

Figure 1(c) shows the charge densities of redispersed microparticle suspensions in which the supernatant solution had been replaced by distilled water. By comparing Figure 1(a) with Figure 1(c), referring also to Figure 1(b), it can be concluded that the main factor affecting the charge properties of SMM suspension is not the residual ions in SMM suspension but the surface charges of SMM particles themselves.

Significant effects of neutralization of $AlCl_3$ prior to microparticle preparation are clearly evident in Figure 1. It is also expected that the increase of Al/Si ratio changes the pH from the basic to the acidic range. It follows that pH is a major factor affecting the change of surface charge properties of SMM microparticles.

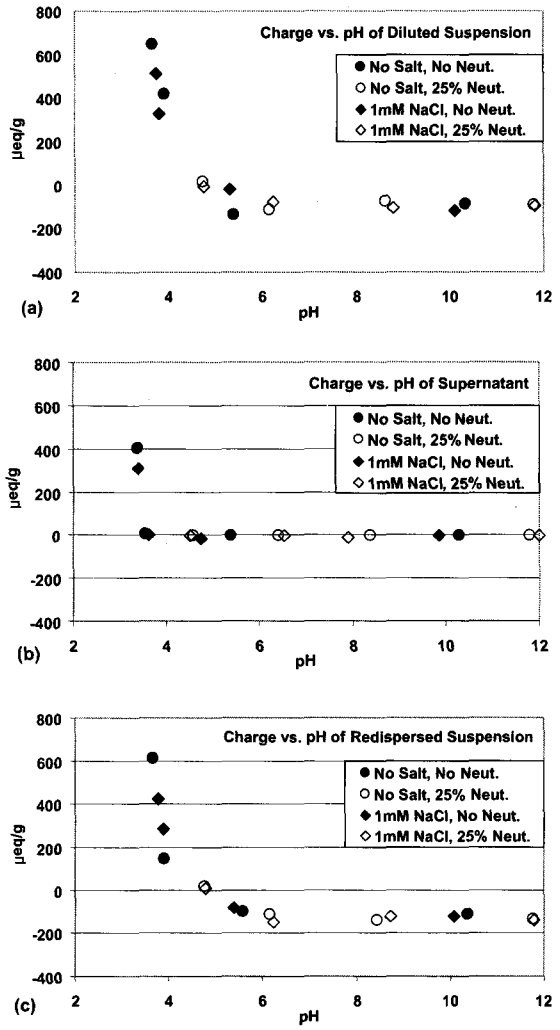

Fig. 2. Charge densities of SMM suspensions, particles, and residual chemicals *vs.* pH: (a) diluted suspension; (b) supernatant; and (c) redispersed suspension.

Surface Charge Densities of SMM and pH

An increase in pH promotes aluminum-III hydrolysis and formation of aluminum-based oligomeric ions [27-28]. Hydrolysis also affects charge and surface properties of both silica particles [29-30] and flocculent species [31]. Lartiges *et al.* observed that the same aluminum dosage yields a lower fraction of aluminum, relative to oxygen, in structures formed at pH 8 than at pH 5.5 [26]. They also noted the formation of a surface gel layer on precipitated silica at high pH [29-30]. This finding suggests also that an enhanced Si/Al reactivity may be responsible for the higher number of aluminosilicate sites found at pH 8 and that deposition of an initial aluminum polymer layer influences the subsequent transfer of other flocculent species to the silica surface. Thereby, the almost neutral flocculent species [31] present at pH = 8 are expected to permit a higher surface coverage of silica particles, giving access to more reaction sites. Otherwise, the highly charged aluminum polycations [31] repel each other and thus limit aluminum incorporation at pH = 5.

The considerations just described help to explain the phenomena in Figure 2. Almost neutralized residual aluminum species in the supernatant show slightly negative charges very near to zero at pH values higher than 5. The aluminosilicate particles in the first redispersed suspension showed lower negative charges at higher pH due to the higher surface coverage of silica particles. There are some critical points where the charges become positive between 4 and 6 in all of 3 graphs in Figure 2. Increasing Al/Si ratio with the increase of the amount of $AlCl_3$ solution during synthesis increases the acidity of the SMM suspension system. This acidity is expected to change the charge properties of Al and Si species on the surface of the microparticles.

Pores of SMM – Effects of Al/Si Ratio and Neutralization

Average pore sizes calculated on a mass basis were found to depend on temperature (Figure 3). Before explaining these data, there are two concepts that need to be introduced.

The first is *destabilization of silica* by polymerized aluminum. An increase in pH promotes aluminum hydrolysis and formation of aluminum-based oligomeric ions. Flocculation of colloidal silica with such ions should begin with the formation of negatively charged aluminosilicate sites. Al_{13} oligomers are expected to either act as counter-ions or to adsorb onto the silica surface after reaction. Thus, these are the principal cations available for charge balance. Aggregation of silica particles with Al_{13} oligomers can then proceed with either charge neutralization or bridging. After that, intercalation of flocculent species between silica particles may explain why the decomposition of Al_{13} oligomers is generally slower than what is observed in solution [26].

The next concept involves the *electrophoretic mobility (EM)* of flocculated particles. Measurements of EM allow

prediction of suspension stability on the basis of electrokinetic characteristics of particles before and after coagulation. Reductions in turbidity of colloidal suspensions have been correlated to charge neutralization, corresponding with good removal of both color and turbidity during water treatment [32].

Figure 4 illustrates the described concept. The dashed line in this figure indicates conditions leading to an electrophoretic mobility of zero. The clouded area corresponds to conditions where aggregation or coagulations can occur. The synthetic conditions of SMM are drawn as straight lines, based on consideration of the amounts of Si and Al added and the pH when it was synthesized. These straight lines cross the line of zero electrophoretic mobility.

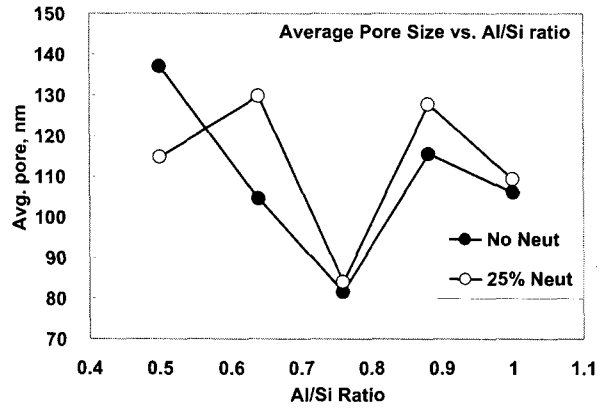

Fig. 3. Effect of Al/Si ratio and neutralization on average pore size and specific surface area calculated by average pore size.

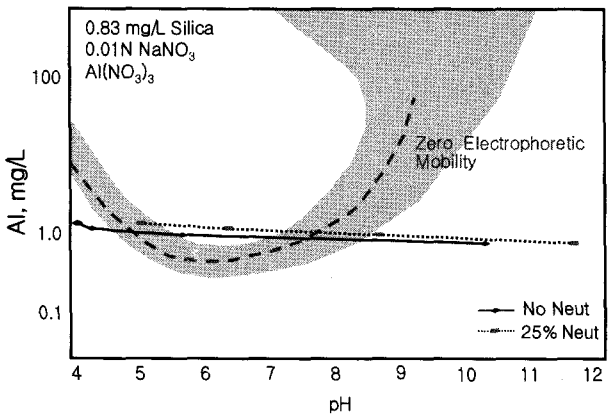

Fig. 4. A scheme of precipitation and charge neutralization model compared with the SMM synthetic conditions of Al amounts and pH [32].

By comparing Figures 3 and 4, it is evident that the average pore sizes and the expected coagulation, as predicted by the electrokinetic measurements, match well in the range of Al/Si from 0.76 to 1.00. It is assumed that the increase of average pore size corresponds to an increase of coagulated structure of SMM particles.

At low Al/Si ratio, where pH values are very high and out of the range of coagulation in Figure 4, the high value of average pore size is explained by the destabilization concept given above. Under strongly alkaline conditions, the hydrolysis of aluminum on the surface of SMM particles is promoted, leading to aggregated structures of SMM particles.

These interpretations were confirmed by the SEM pictures.

Morphology of SMM with SEM

The sample in Figure 5 was filtered to remove water. It is apparent from the figure that SMM does not consist of homogeneous particles. The image shows relatively large, fused structures, in addition to assemblages of well-identifiable primary particles. Nano-scale solid features and pores can be seen. In summary, the SMM system in aqueous solution appears to exist as fused structures which themselves consist of various sizes of particles.

Changes in the state of agglomeration of the microparticles, depending on pH variations, are shown in Figure 6. As the Al/Si ratio increased, the SMM particles appeared to become more uniformly distributed. Further increase in the ratio appeared to increase agglomeration again, an effect that may be associated with the decrease of pH.

When the pictures are compared horizontally, effects of neutralization are evident. Neutralization makes the systems less acidic. However, this less acidity doesn't mean more distribution. Based on Figures 3 and 4, when the pH of neutralized sample is near to zero electrophoretic mobility, one can expect the structure to be more fused.

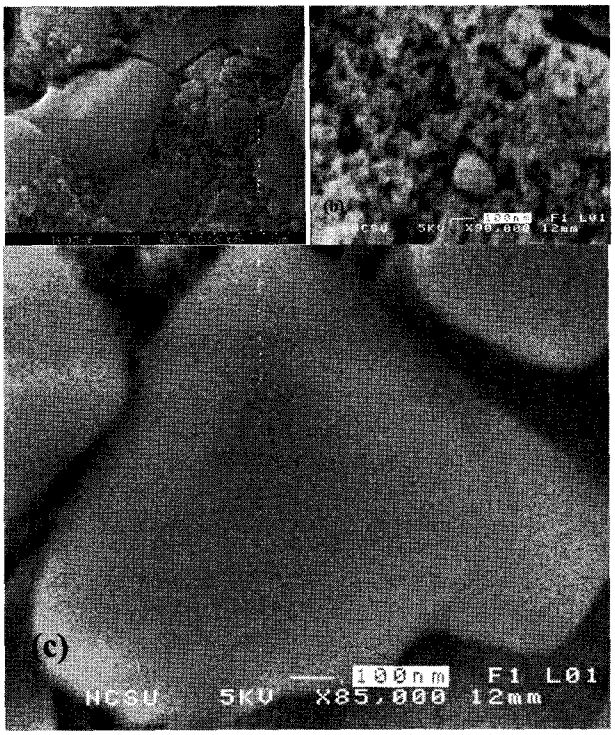

Fig. 5. SEM pictures of filtered thick samples; Al/Si = 0.63, 13,000 rpm, No Neutralization.

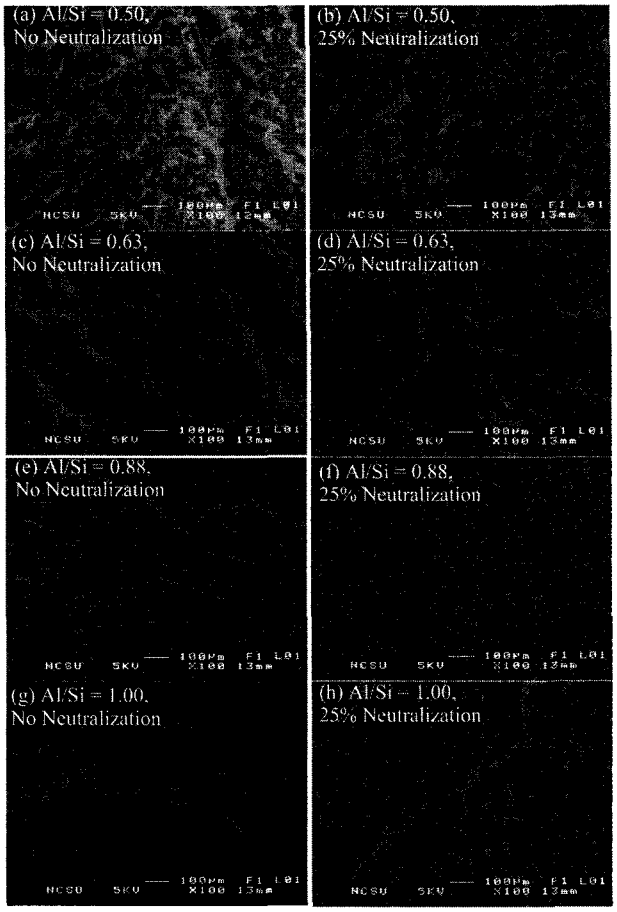

Fig. 6. Fused behavior of SMM depending on Al/Si ratio and neutralization.

CONCLUSIONS

The change of pH caused by increasing Al/Si ratio with the increase of the amount of $AlCl_3$ solution during synthesis affects the charge properties of SMM particles due to Al and Si species on the surface of the microparticles.

Considering destabilization of silica by polymerized aluminum as well as electrophoretic mobility of flocculated particles, pH was explained as the major factor to control pore size, particle size and fused behavior of SMM

REFERENCES

[1] Hubbe, M. A., *Micro and Nanoparticles in Papermaking*, Ed. Rodriguez, Ch. 1,TAPPI Press (2005).
[2] Langley, J. G. and Litchfield , E., *Proc. TAPPI 1986 Papermakers Conf.*, 89 (1986).
[3] Litchfield, E., *Appita 47* (1): 62 (1994).
[4] Langley, J., and Holroyd, D., *U. S. Pat. 4,753,710*, June 28 (1988).
[5] Knudson, M. I., *Proc. TAPPI Papermakers Conf.*, 141 (1993).
[6] Iler, R. K., The Chemistry of Silica – Solubility, Polymerization, Colloid and Surface Properties, and Biochemistry, J. Wiley & Sons, (1979).
[7] On, C., and Thorn, I., *Eur. Papermaker 3* (2): 28 (1995)
[8] Suden, O., Båtelson, P. G., Johansson, H. E., Larsson, H. M., and Svending, P. J., *U. S. Pat. 4,388,150*, June 14 (1983)
[9] Rushmere, J. D., *U. S. Pat. 4,954,220*, Sept. 4 (1990).
[10] Harms, M., *Wochenbl. Papierfabr. 126* (19): 922 (1998).
[11] Honig, D. S., Harris, E. W., Pawlowska, L. M., O'Toole, M. P., and Jackson, L. A., *TAPPI J. 76* (9): 135 (1993).
[12] Andersson, K., Larsson, B., and Lindgren, E., *U.S. Pat. 5,603,805*, Feb. 18 (1997).
[13] Honig, D. S., Farinato, R. S., and Jackson, L. A., *Nordic Pulp Paper Res. J. 15* (5): 536 (2000).
[14] Aloi, F. G., and Trksak, R. M., *Retention of Fines and Fillers during Papermaking*, Ed. Gess, J. M., 61-108 TAPPI Press (1998).
[15] O'Brien, J. A., Lawrence, L. A., and Honig, D. S., *Proc. TAPPI 1994 Papermakers Conf.*, 257 (1994).
[16] Drummond, D. K., *U.S. Pat. 6,184,258 B1*, Feb. 6 (2001).
[17] Drummond, D. K., *U.S. Pat. 5,989,714*, Nov. 23 (1999).
[18] Drummond, D. K., *U.S. Pat. 6,183,650 B1*, Feb. 6 (2001).
[19] Gane, P. A. C., Ridgway, C. J., Lehtinen, E., Valiullin, R., Furó, I., Schoelkopf, J., Paulapuro, H., and Daicic, J., *Ind. Eng. Chem. Res. 43* (24): 7920-7927 (2004).
[20] Ishikiriyama, K., Todoki, M., and Motomura, K., *Journal of Colloid Interface Science, 171* (1): 92-102 (1995).
[21] Park, S., Venditti, R. A., Jameel, H., and Pawlak, J. J., Accepted to *Carbohydrate Polymers* on Feb. 2006.
[22] Luukkonen, P., Maloney, T. C., Rantanen, J., Paulapuro, H., and Yliruusi, J., *Pharmaceutical Research 18* (11): 1562-1569 (2001).
[23] Maloney, T. C., Paulapuro, H., and Stenius, P., *Nordic Pulp and Paper Research Journal, 1 3*(1): 31-36 (1998).
[24] Furó, I. and Daicic, J., *Nordic Pulp Paper Res. J., 14* (3): 221-225 (1999).
[25] Nakamura, K., Hatakeyama, T., and Hatakeyama, H., *Textile Res. J., 51* (9): 607-613 (1981).
[26] Lartiges, B. S., Bottero, J. Y., Derrendinger, L. S., Humbert, B., Tekely P., and Suty, H., *Langmuir 13* (2): 147 (1997).
[27] Bottero, J. Y., Tchoubar, D., Cases, J. M., Fiessinger F., *Journal of Physical Chemistry 86* (18): 3667 (1982).
[28] Bottero, J. Y., Cases, J. M., Fiessinger, F., Poirier, J. E., *Journal of Physical Chemistry 84* (22): 2933 (1980).
[29] Axelos, M. A. V., Tchoubar, D., Bottero, J. Y., *Langmuir 5* (5): 1186 (1989).
[30] Vigil, G., Xu, Z., Steiberg, S., Israelachvili, J., *Journal of Colloid and Interface Science 165* (2): 376 (1994).
[31] Furrer, G., Ludwig, C., Schindler, P. W., *Journal of Colloid and Interface Science 149* (1): 56 (1992).
[32] Dentel, S. K., *Environmental Science and Technology 22*:825-832 (1988)